Proceedings of the 21st ICSMGE, Vienna, Austria, 14 – 19 June 2026. Pistrol, Adam & Schweiger (eds.)
Published by: ÖGG, Austrian Society for Geomechanics, Salzburg, Austria, ISBN 978-3-9503898-4-5
https://doi.org/10.53243/ICSMGE2026-1471

Modelling of control piles deformable cells mechanical behavior based on uniaxial compression tests

Rodrigo Rodríguez, Marco Pérez, Carlos Sánchez, Dario Armendáriz, Rubén Domínguez-Alfaro, Gabriel Auvinet.
Institute of Engineering of UNAM, Mexico City, Mexico, rrodriguezr@iingen.unam.mx

ABSTRACT: The subsoil of Mexico City is affected by the overexploitation of its aquifers, which causes a drawdown of pore pressure and, consequently, regional subsidence (RS) and differential settlements in many structures across the city. In 1948, González-Flores introduced the control pile system to allow buildings that tend to exhibit apparent uplift to follow the RS. The system generally consists of a pile, a load-bearing frame connected to the slab by studs, and a deformable cell composed of wooden cube arrangements located between the pile head and the load-bearing frame. Several studies have examined the mechanical behavior of materials used as deformable cells in control piles through uniaxial compression tests (López-Acosta and Martínez, 2017). This study aims to identify the constitutive law that best represents the behavior of different deformable cell configurations, based on laboratory test results and calibrated using the PLAXIS SoilTest module.

KEYWORDS: Deep foundation, control piles, deformable cells, laboratory tests, constitutive law.

1 INTRODUCTION

1.1 *Regional subsidence*

The subsoil of Mexico City is subject to aquifer overexploitation, which leads to a reduction in pore water pressures and, consequently, induces regional subsidence (RS). Nearly a century after its initial recognition by Roberto Gayol (1925) and more than seventy years after its interpretation by Nabor Carrillo (1947), RS continues to affect the city, causing differential settlements in numerous structures. These deformations result in several impacts, including damage to underground lining systems, apparent uplift of structures with deep or overcompensated foundations, and ground cracking in transition zones, all of which pose potential hazards.

Despite considerable efforts, RS has not been successfully controlled, making it necessary to implement urgent measures to preserve affected structures and to reconsider strategies for mitigating future effects. Figure 1 illustrates the spatial variability of subsidence rates, with observations indicating that some areas of Mexico City have experienced values approaching 40 cm/year.

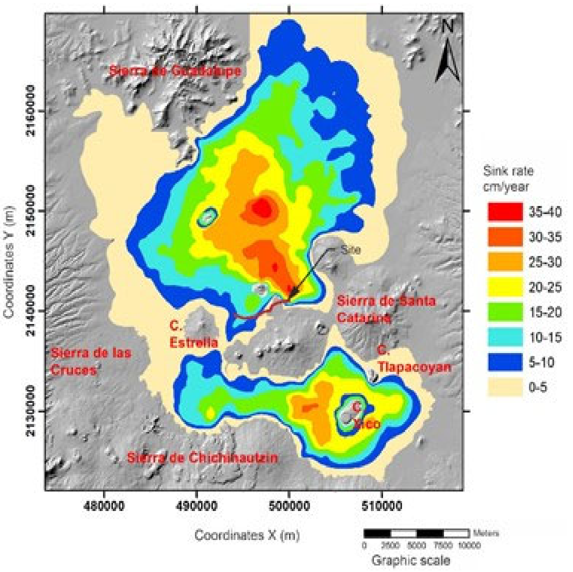

Figure 1. Mapping of rates of regional subsidence (Juárez *et al*., 2022)

1.2 *González-Flores 1948*

In 1948, González Flores developed a special type of foundation that, for its time, represented an innovative solution to the problems associated with regional subsidence. Three years later, he obtained a patent for the system. It was initially conceived as an alternative for underpinning buildings affected by phenomena such as apparent uplift and differential settlements; however, its application was later extended to new foundation systems (see Figure 2).

In general terms, a control pile consists of three main components:

1. The pile, either end-bearing or friction type, which transfers loads to the bearing stratum or to a significant thickness of soil.
2. The load frame or bridge, hinged to the foundation slab, which receives the portion of structural load assigned to it and transfers it to the pile.
3. The deformable cell, a package approximately 15 cm in height composed of an arrangement of caobilla wood blocks, whose controlled crushing regulates the load transmitted to the pile and allows millimetric adjustments of the structure's elevation.

It is known that approximately 700 buildings in Mexico City incorporate the control pile system. Notable examples include the Templo de las Capuchinas (adjacent to the old Basilica of Guadalupe), the Camino Real Aeropuerto Hotel (in front of Terminal 1 of the Benito Juárez International Airport), and the former Ministry of Foreign Affairs building in Tlatelolco (PICOSA, 2010).

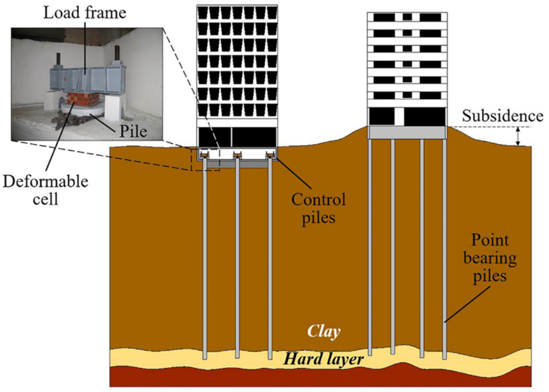

Figure 2. Solution to the regional subsidence by means of the control piles (López-Acosta *et al*., 2020)

2 DESCRIPTION OF CONTROL PILES

2.1 *The pile*

Piles used in underpinning works may be made of steel or reinforced concrete, generally with a circular cross section and assembled from 91 cm (3 ft) Mega-type segments (Santoyo and Alanís, 2013). Their diameter, depth, and the type and amount of reinforcement are determined according to the specific design conditions of each foundation, considering factors such as static and dynamic loads, the depth of the caisson foundation, and the geotechnical properties of the soil. The most common models have diameters of 45 cm, with an approximate load capacity of 100 t, and 60 cm for capacities of about 150 t (PICOSA, 2010). To ensure verticality during installation, a predrilling operation is performed until reaching the bearing stratum.

2.2 *Load frame*

The load frame, originally proposed by González-Flores (1948), consists of a steel head with screws or threaded rods at its ends, which are anchored to steel supports located at the lower part of the system. These supports are embedded in and structurally connected to the bottom slab of the caisson foundation through reinforcing bars known as anchors. To improve seismic stability, two concrete stabilizers one at each end were incorporated into the original design (Santoyo and Alanís, 2013).

2.3 *Deformable cell*

The deformable cell is placed between the pile head and the load frame and is an essential component of the system. Its primary function is to transmit a constant load to the pile while deforming at the same rate as regional subsidence, allowing controlled settlement of the structure and maintaining soil–structure contact.

González-Flores originally proposed using a material with perfectly elastic–plastic behavior, characterized by a plastic behavior factor (*Fcp*) equal to one, such that the pile would operate under a constant load once yielding occurred. Initially, mahogany blocks were used, but these were later replaced by caobilla wood due to its lower cost and similar mechanical properties.

The deformable cell typically consists of wooden cubes measuring 5 cm per side, arranged in three layers and separated by galvanized steel plates. Its total height is 15 cm, plus approximately 2 mm corresponding to the steel plates (Santoyo and Alanís, 2013). Figure 3 illustrates all components of a control pile system.

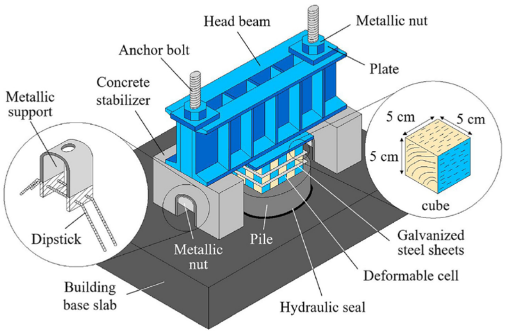

Figure 3. Components of the traditional control pile system (López-Acosta *et al*., 2020)

2.4 *Wooden blocks arrangements*

González Flores proposed the use of three layers of wooden blocks to provide sufficient deformation capacity before requiring readjustment of the load frame. He also ingeniously incorporated galvanized steel plates between the layers to ensure that the cubes in all three layers would deform in a uniform manner. Figure 4 shows the deformation patterns of two columns of three cubes with the wood grain oriented horizontally one including steel plates between layers and the other without them. The contrast is significant and demonstrates that omitting the plates constitutes a maintenance error.

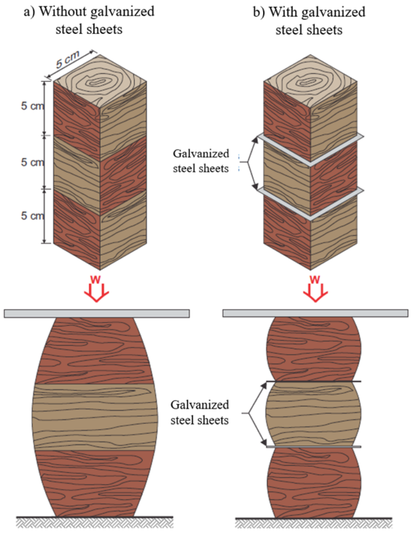

Figure 4. Deformation patterns of wooden cubes tested with horizontal thread with and without sheet separations (Santoyo and Alanís, 2013)

The criterion for replacing crushed cubes varies; however, considering that the plastic deformation limit of wood is approximately 30%, and that beyond this threshold the cross-sectional area increases thereby raising its load-carrying capacity it is recommended to replace the cubes when the load frame (bridge) has descended by about 5 cm. Replacing the cubes requires lifting the bridge to restore the original height corresponding to the new cubes, as well as compensating for the emergence of the pile.

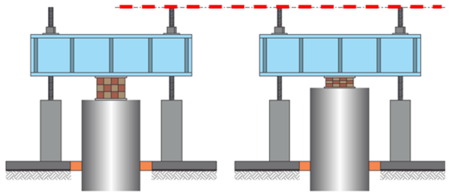

a) Initial condition b) The wooden cubes are crushed.

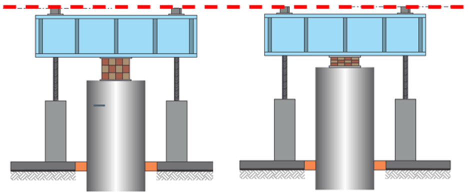

c) The wooden cubes are replaced. d) The wooden cubes are crushed and when there is no more space, the pile is cut down.

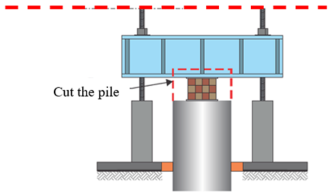

e) The pile is trimmed, and the control continues

Figure 5. Example of a pile cutting case (Santoyo and Alanís, 2013)

3 STUDY OF THE MECHANICAL BEHAVIOR OF WOODEN CUBES (LÓPEZ-ACOSTA AND MARTÍNEZ HERNÁNDEZ, 2017)

3.1 *Previous studies*

The load capacity of deformable cells composed of wooden cubes has primarily been estimated through tests performed on individual blocks.

González-Flores did not publish formal experimental results; however, in his underpinning projects he estimated average capacities of 25 kN (González-Flores, 1959) and later proposed a yield limit of 29 kN (González-Flores, 1964).

Salazar-Resines (1978) carried out controlled-deformation tests and concluded that statistical analysis was necessary to classify the cubes and achieve more uniform deformation behavior.

Aguilar and Rojas (1990) tested 20 cubes randomly selected from a batch of 5000 and determined that the wood exhibits perfectly plastic behavior, with deformations ranging from 10% to 30% and an average strength of 25 kN, with a standard deviation of ±5 kN.

Santoyo and Segovia (1995) reported strengths ranging from 25 to 34 kN, reflecting the heterogeneity of the material, and observed that the compressive strength decreases by 40% in the wet state, eliminating the plasticizing capacity. Tests on cubes from the Metropolitan Cathedral revealed that some reached plasticization at a deformation of 0.15 cm.

3.2 *Study of individual and combined wooden cubes (López-Acosta and Martínez Hernández, 2017)*

The authors evaluated the mechanical behavior of deformable cells used in control piles through unconfined compression tests conducted on both individual cubes and assembled configurations. The tests were performed using a hydraulic universal testing machine with a maximum capacity of 2452 kN (Figure 6).

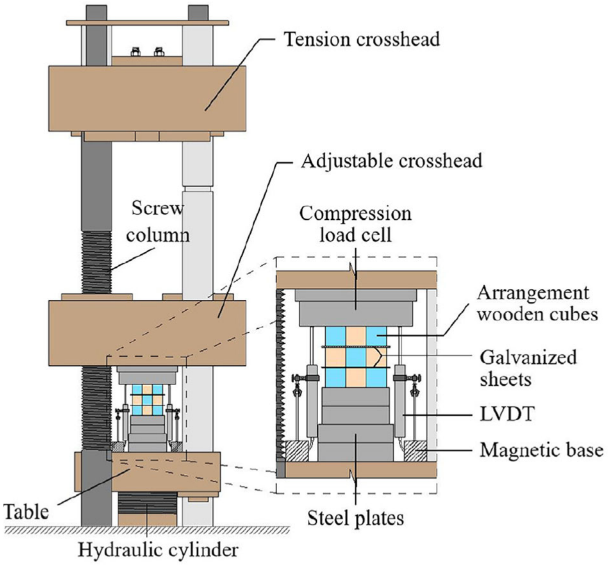

Figure 6. Test equipment and measurement instruments (López-Acosta *et al*., 2020)

A total of 56 tests were performed using 876 wooden cubes with 5 cm sides. The unit weight of the cubes showed high variability, ranging from 4064 kN/m³ to 7662 kN/m³. Based on a statistical analysis of 665 cubes (from a total sample of 1500), an average unit weight of 5588 kN/m³ was obtained. Using this criterion, cubes were classified as light or heavy when their unit weight was below or above the average, respectively.

Based on this classification, various arrangements were assembled using heavy cubes, light cubes, and mixed configurations. Galvanized steel sheets 1.5 mm thick were included in the three-layer arrangements, with each layer composed of 3×3, 4×4, 5×4, and 8×7 cube configurations. Table 1 presents the test characteristics and the number of tests performed.

Table 1. Laboratory tests performed on caobilla wood cubes

Description	GSS	Loading of tests (kN/min)	Number of tests
Individual dry cubes (FOV)	-	5	5
Individual dry cubes (FOH)	-	5	30
Individual wet cubes (FOH)	-	5	9
Three level arrangements 3 x 3	Yes	20	5
Three level arrangements 3 x 3	No	20	3
Three level arrangements 4 x 4	Yes	20	3
Three level arrangements 5 x 4	Yes	20	2
Three level arrangements 8 x 7	Yes	20	1

Here, **FOV** refers to wood fibers oriented vertically, **FOH** to fibers oriented horizontally, and **GSS** to galvanized steel sheets. Figure 7 presents the stress–strain curves for a three-layer 3×3 arrangement with galvanized steel plates, tested using heavy, standard, and light cubes.

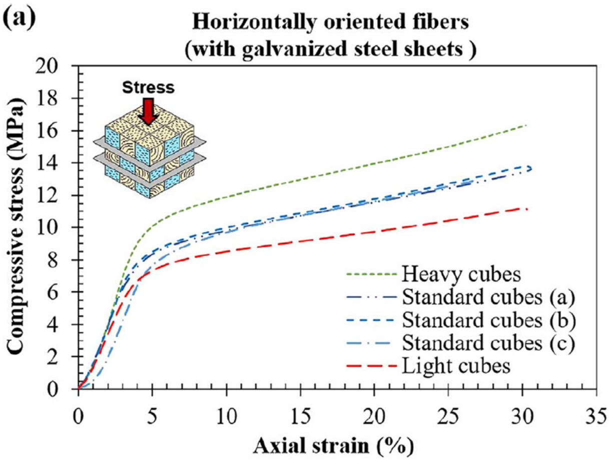

Figure 7. Mechanical behavior of three-level arrangements of 3 x 3 cubes with galvanized steel sheets (López-Acosta *et al*., 2020)

4 NUMERICAL REPRESENTATION OF THE DEFORMABLE CELL OF WOODEN CUBES

4.1 *Hardening soil model (HS)*

Based on the experimental results, *caobilla* wood cubes exhibit elastoplastic behavior with hardening, as shown in Figure 7. The Hardening Soil (HS) model is an advanced constitutive model derived from elastoplastic soil mechanics with hardening, capable of representing the nonlinear behavior of geomaterials under loading and unloading. The model accounts for different stiffness values corresponding to various strain conditions (Figure 8).

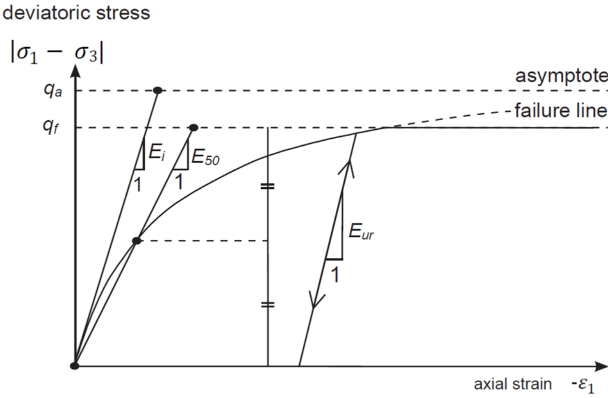

Figure 8. Hyperbolic stress-strain relation in primary loading for a standard drained triaxial test (Plaxis 2D, 2024.3)

4.2 *PLAXIS SoilTest*

In PLAXIS, SoilTest is an integrated tool used to simulate and calibrate the behavior of a material before incorporating it into a full geotechnical model.

It essentially functions as a virtual laboratory in which different tests can be reproduced and material parameters adjusted until the numerical response matches the laboratory results. In this study, the tool was used to simulate an unconfined triaxial test, as illustrated in Figure 9.

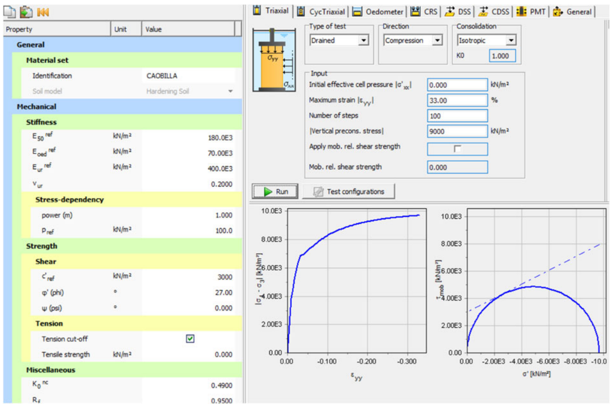

Property	Unit	Value
General		
Material set		
Identification		CAOBILLA
Soil model		Hardening Soil
Mechanical		
Stiffness		
$E_{50}{}^{ref}$	kN/m²	180.0E3
$E_{oed}{}^{ref}$	kN/m²	70.00E3
$E_{ur}{}^{ref}$	kN/m²	400.0E3
ν_{ur}		0.2000
Stress-dependency		
power (m)		1.000
p_{ref}	kN/m²	100.0
Strength		
Shear		
c'_{ref}	kN/m²	3000
φ' (phi)	°	27.00
ψ (psi)	°	0.000
Tension		
Tension cut-off		☑
Tensile strength	kN/m²	0.000
Miscellaneous		
$K_0{}^{nc}$		0.4900
R_f		0.9500

Type of test: Drained
Direction: Compression
Consolidation: Isotropic
K0: 1.000

Input
Initial effective cell pressure $|\sigma'_{xx}|$: 0.000 kN/m²
Maximum strain $|\varepsilon_{yy}|$: 33.00 %
Number of steps: 100
|Vertical precons. stress|: 9000 kN/m²
Apply mob. rel. shear strength: ☐
Mob. rel. shear strength: 0.000

Figure 9. Numerical simulation to represent a uniaxial compression test (Plaxis 2D, 2024.3)

4.3 *Simulation of laboratory results with PLAXIS SoilTest*

This work began in 2023 at the Geoinformatics Laboratory of the Institute of Engineering of UNAM (II-UNAM). The laboratory tests reported by López-Acosta and Martínez Hernández (2017) were numerically simulated using the PLAXIS SoilTest module.

The following figures present the calibrated curves comparing laboratory (Lab) and numerical (Num) results. Figure 10 shows the response of individual light and heavy cubes in dry conditions, with wood fibers oriented horizontally. Figure 11 presents the response of individual light and heavy cubes in wet conditions, also with horizontal fiber orientation. Figure 12 corresponds to a three-layer 3×3 arrangement with galvanized steel sheets, including both light and heavy cubes. Figure 13 shows a three-layer 3×3 arrangement without galvanized steel sheets, likewise including light and heavy cubes.

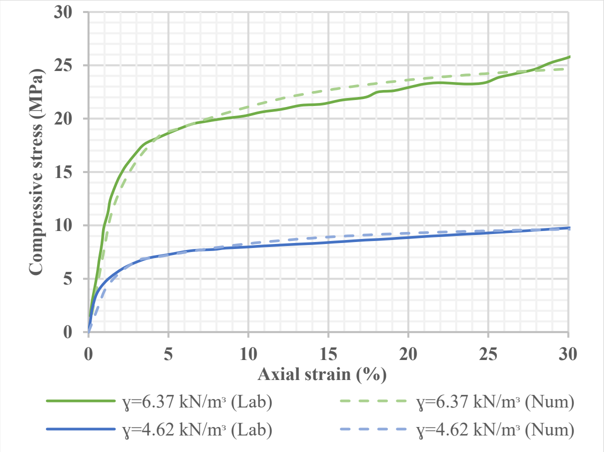

Figure 10. Individual dry wooden cubes (heavy and light) with horizontally oriented fibers.

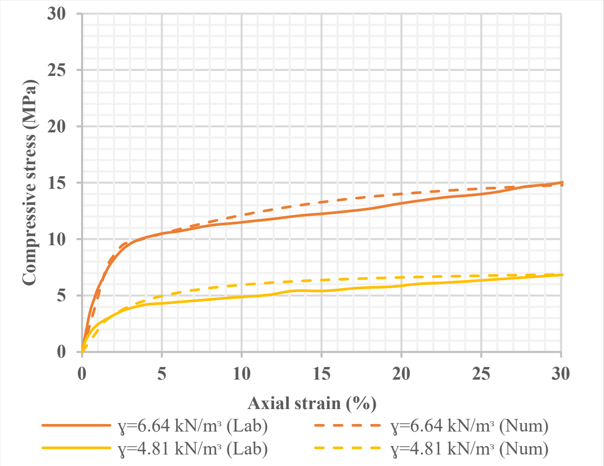

Figure 11. Individual wet wooden cubes (heavy and light) with horizontally oriented fibers

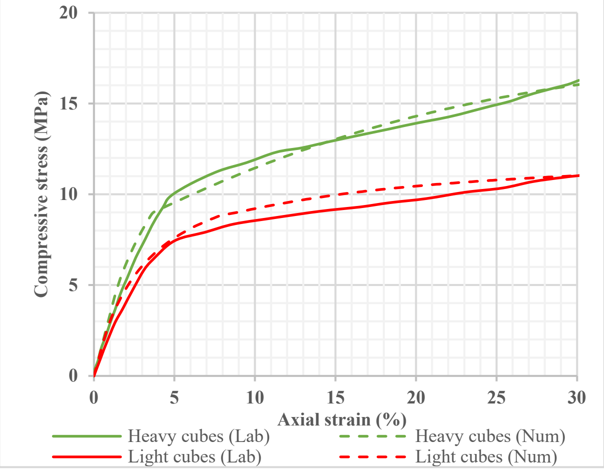

Figure 12. Three-layer 3×3 cube arrangements with galvanized steel sheets

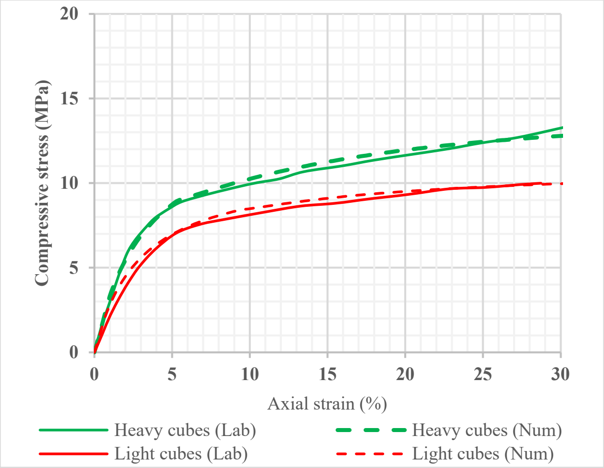

Figure 13. Three level arrangements of 3 x 3 cubes without galvanized steel sheets

Table 2 presents the parameters obtained from the calibration corresponding to each graph. Columns 1 and 2 correspond to the curves of individual dry cubes (heavy and light). Columns 3 and 4 correspond to the curves of individual wet cubes (heavy and light). Columns 5 and 6 present the results for the three-layer 3×3 arrangement with galvanized steel sheets (heavy and light cubes), while Columns 7 and 8 correspond to the three-layer 3×3 arrangement without galvanized steel sheets.

In this same table, c' denotes the effective cohesion, φ' the effective friction angle, E_{50}^{ref} the secant stiffness in a standard drained triaxial test E_{eod}^{ref} the tangent stiffness for primary loading in the oedometer, E_{ur}^{ref} the unloading/reloading stiffness, v'_{ur} the Poisson's ratio for unloading/reloading, p_{ref} the reference stress for the stiffnesses, R_f the failure ratio q_f / q_a, m the exponent for the stress-level dependency of stiffness y K_0^{nc} the coefficient of earth pressure at rest for normally consolidated conditions.

Table 2. Mechanical parameters based on calibration

Parameters	1	2	3	4	5	6	7	8
c' (MPa)	8.0	3.0	4.9	2.3	6	3.8	4.5	3.4
φ' (º)	27	27	25	25	25	24	24	24
E_{50}^{ref} (MPa)	400	180	250	100	170	160	170	155
E_{eod}^{ref} (MPa)	160	70	83	40	83	83	83	83
E_{ur}^{ref} (MPa)	800	400	500	200	340	320	340	310
v'_{ur}	0.2	0.2	0.2	0.2	0.2	0.2	0.2	0.2
p_{ref} (kPa)	100	100	100	100	100	100	100	100
R_f	0.98	0.95	0.95	0.95	0.95	0.95	0.95	0.95
m	1.0	1.0	1.0	1.0	1.0	1.0	1.0	1.0
K_0^{nc}	0.49	0.49	0.49	0.49	0.49	0.49	0.49	0.49

4.4 *Numerical representation of the control pile system*

In 2024, Domínguez-Alfaro presented the results of a numerical assessment of the behavior of a group of control piles. Three-dimensional models of a box foundation with different control pile configurations were developed. In these models, the piles, loading frames, and deformable cells were explicitly represented (Figure 14).

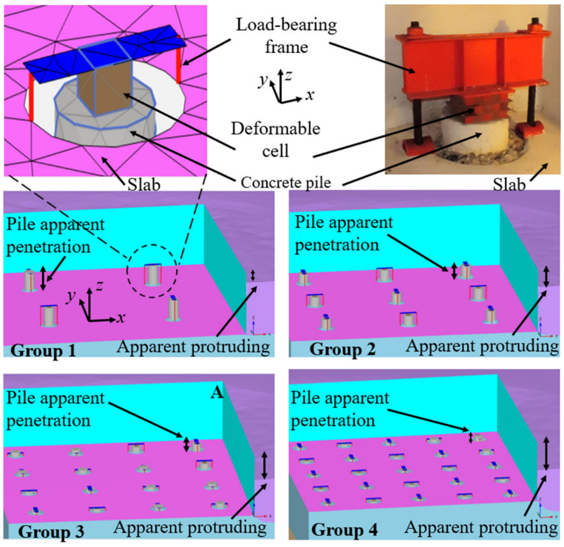

Figure 14. Numerical model of foundation with control piles (Domínguez-Alfaro, 2024)

To model the deformable cell, the calibration criteria obtained using PLAXIS SoilTest and the Hardening Soil (HS) constitutive model were applied. A three-level deformable cell consisting of a 4 × 4 arrangement of cubes was represented using a single volume element (Figure 15).

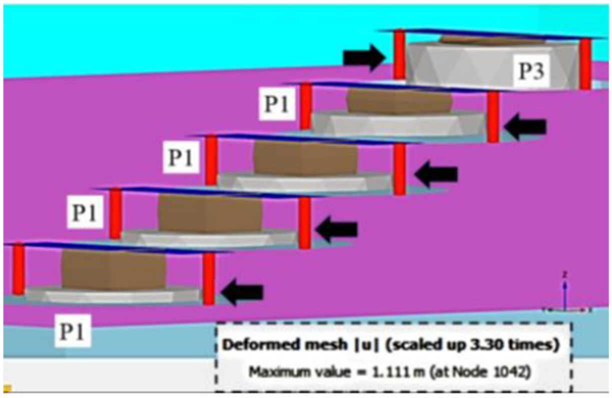

Figure 15. Numerical model of deformable cell (Domínguez-Alfaro, 2024)

5 CONCLUSIONS

Control piles are a type of special foundation, attributed to González Flores (1948), designed to mitigate the effects of regional subsidence in buildings exhibiting apparent protrusion and tilting.

The deformable cell is a fundamental component of this system, as it plays a key role in the proper performance of the structures that employ it. This work presents a numerical calibration based on unconfined compression tests conducted in the laboratory, in which wooden cubes with different configurations were analyzed.

Using PLAXIS and the SoilTest tool, the laboratory results were accurately reproduced with the Hardening Soil constitutive model. In this study, only individual cubes dry and wet, heavy and light and three-level cells with 3 × 3 cube arrangements, both with and without galvanized steel sheets, were calibrated.

Based on this calibration criterion, the three-dimensional model can be optimized by representing the deformable cell with a single volume element that preserves the real dimensions of the cell, without the need to model each cube individually or explicitly incorporate the galvanized steel sheet.

At II-UNAM, ongoing research continues to focus on calibrating additional configurations of deformable cells.

6 REFERENCES

Aguilar, J. y Rojas, E. (1990) “Importantes mejoras en los dispositivos de control de pilotes”, XV Reunión nacional de mecánica de suelos. Sociedad Mexicana de Mecánica de suelos. México.

Auvinet, G., Méndez, E. y Juárez, M. (2016). El subsuelo de la Ciudad de México/The subsoil of Mexico City, Vol. III, ISBN 978-607-02-8198: UNAM.

Bentley Systems International Limited. (2024). Manual de referencia de PLAXIS 2D/3D CONNECT Edition V24 [Manual de software]. bentleysystems.service-now.com

Carrillo, N. (1948). “Influence of Artesian Wells on the Sinking of México City”, Proceedings, Second International Conference on Soil Mechanics and Foundation Engineering, Vol. 2, pp 156-159, Rotterdam, Netherlands.

Domínguez-Alfaro, R. (2024). “*Evaluación numérica del comportamiento en grupo de pilotes de control*”. National Autonomous University of Mexico. Master thesis. Mexico.

Gayol, R. (1925). “Estudio de las perturbaciones que en el fondo del Valle de México ha producido el drenaje de las aguas del subsuelo …”, Primera parte, Revista Mexicana de Ingeniería y Arquitectura, Vol. III, No. 3, pp. 96-132, México, agosto 1925.

Juárez, M., Auvinet, G., Román, H., y Méndez, E. (2022) “Predicción del hundimiento regional en el valle de México” XXXI Reunión nacional de Ingeniería Geotécnica. Guadalajara, México.

López-Acosta, N. y Martínez, E. (2017) “Capitulo 6 Pilotes de control” En Ingeniería de cimentaciones profundas. Vol. II, Sociedad Mexicana de Ingeniería Geotécnica.

López-Acosta, N. y Martínez, E. (2019) “Underpinning and releveling of a building using control piles and sub-excavation”, Proceedings of the XVI Pan-American conference on Soil Mechanics and Geotechnical Engineering. México.

López-Acosta, N. *et al.,* (2020) “Mechanical Characterization of deformable cells in control piles” Soil and Foundations, 60, 139-154. http://doi.org/10.1016/j.sandf2020.01.006

López-Acosta, N. y Martínez, E. (2021) “Pilotes de control: funcionamiento, diseño y aplicación” (SID 710). Instituto de Ingeniería. UNAM. México.

Martínez, E. (2017) “Estudio del comportamiento mecánico de materiales empleados como celdas de deformación en el sistema de pilotes de control.”. Tesis de Maestría. UNAM.

Martínez, E., López-Acosta, N., Espinosa, A. y Barba, D. (2023) “Instrumentación geotécnica en pilotes de control, estudio de un caso práctico”. VI Simposio Internacional de Cimentaciones Profundas, México.

PICOSA. (2010) “Ecuaciones para el diseño de capacidad de carga de González Flores” Informe proporcionado por Pilotes de control S.A. de C.V. México.

PICOSA. (2014) “Cimentando a México desde 1951” Pilotes de control S.A. de C.V. Al Instituto de Ingeniería. México.

PICOSA. (2015) “Patente No. 328256: Pilote de control con elemento deformable para cimentar, recimentar y/o renivelar edificios y conservarlos conforme a su diseño original” Instituto Mexicano de la Propiedad Industrial.

Salazar, J. (1960) “Control of loads and settlements of buildings by means of mechanisms attached to the piles”. Proceedings of the 1ST Pan-American Conference on Soil Mechanics and Foundation Engineering. Vol. 1. Mexico City.

Santoyo, E., y J. A. Segovia (1995). Recimentación y renivelación de estructuras y monumentos: 26. México: TGC.

Santoyo E. y Alanís R. (2013) “Monografía sobre los pilotes de control: utilidad, mantenimiento y desatinos”. México.